

# CrystEngComm

Accepted Manuscript



This is an *Accepted Manuscript*, which has been through the Royal Society of Chemistry peer review process and has been accepted for publication.

*Accepted Manuscripts* are published online shortly after acceptance, before technical editing, formatting and proof reading. Using this free service, authors can make their results available to the community, in citable form, before we publish the edited article. We will replace this *Accepted Manuscript* with the edited and formatted *Advance Article* as soon as it is available.

You can find more information about *Accepted Manuscripts* in the [Information for Authors](#).

Please note that technical editing may introduce minor changes to the text and/or graphics, which may alter content. The journal's standard [Terms & Conditions](#) and the [Ethical guidelines](#) still apply. In no event shall the Royal Society of Chemistry be held responsible for any errors or omissions in this *Accepted Manuscript* or any consequences arising from the use of any information it contains.



Journal Name

ARTICLE

## Temperature dependence of the photoluminescence from ZnO microrods prepared by a float zone method†

Xingyuan Guo,<sup>a</sup> Carl P. Tripp,<sup>b</sup> Changfeng Chen,<sup>b</sup> Yan Wang<sup>c</sup> Shengyan Yin<sup>d</sup> and Weiping Qin<sup>\*d</sup>

Received 00th January 20xx,  
Accepted 00th January 20xx

DOI: 10.1039/x0xx00000x

www.rsc.org/

A facile float zone method to grow ZnO microrods with hexagonal crystal structure is described. It was found that the crystal-growth mechanism was different from the well-known vapor-liquid-solid (VLS) growth mechanism. However, the one-dimensional growth morphologies occurring in the vapor phase is similar to ZnO grown using conventional VLS processes. The free-exciton, bound-exciton, acceptor-exciton, two-electron satellite emission, and its phonon replica, obtained from the 15 K photoluminescence (PL) spectra of ZnO microrods were recorded. The PL spectra of ZnO microrods at temperatures between 15 and 150 K show that the bound-exciton peak dissociates into a free-exciton peak and that the free-exciton emission and its phonon replicas dominate at temperatures above 120 K. Following the approach of Viswanth for measuring the intensity ratio of PL peaks, we found that the strongest bound exciton peak at 3.3615 eV had a thermal activation energy of 15.9 meV, consistent with the value expected for the exciton-defect binding energy. This bound-exciton peak was not observed at temperatures above 120 K.

### 1. Introduction

Zinc oxide is an attractive semiconductive material because it has a direct wide band gap of 3.37 eV and a strong excitonic binding energy of 60 meV at room temperature. These properties are of particular importance when developing UV light-emitting diodes and laser diodes with high emitting efficiency.<sup>1</sup> In particular, microstructured ZnO possessing a hexagonal crystal structure has drawn considerable interest for use in optical resonators due to their unique, well-defined geometry and excellent optical properties.<sup>2,3</sup> It is expected that the low lasing threshold and the high quality factor Q are a result of a highly efficient exciton emission, due to the carrier confinement inside the microcavity and total internal reflections at the interface of the resonator boundaries. These properties have, for example, led to Fabry-Perot mode lasing and whispering gallery mode lasing.<sup>4,6</sup> However, despite efforts to optimize or control the growth of ZnO microrods, there are few examples of single-crystalline microstructures with longer than tens of  $\mu\text{m}$  reported.<sup>6-8</sup> In addition, few studies have addressed the low temperature and temperature dependent PL of ZnO microrods.<sup>9-11</sup>

In this work, we report the synthesis of ZnO microrods with a

hexagonal crystal structure using a float zone (FZ) method. The evolution of the variable temperature PL of free-exciton (FX), neutral-donor-bound-exciton ( $D^0X$ ) emission and its phonon-replica over the temperature range of 15-150 K was also measured. There are similarities between the ZnO microrods grown using the FZ methods and those described by a vapor-liquid solid (VLS) growth mechanism,<sup>12</sup> in that we obtain one-dimensional growth morphologies, and that growth occurs through a reaction with a vapor precursor. However, it is noted that the FZ method is suitable for growing high melting point single crystal materials that do not require reaction with a vapor precursor, such as is found with the preparation of  $\text{TiO}_2$ ,  $\text{BaTi}_2\text{O}_5$ .<sup>13,14</sup> In the case of the ZnO microrods produced with the FZ method, the vapor reaction introduces experimental difficulties associated with the deposition of materials on components within the furnace.

### 2. Experimental procedure

ZnO powders (99.8% purity) were packed into a rubber cylindrical tube sealed at one end. The tube was 1 cm in diameter and 10 cm in length. The filled tube was evacuated for 10 min using a mechanic pump attached to the open end of the tube. The tube was then compressed for 5 minutes under a hydrostatic pressure of 60 MPa to form ZnO rods that were 5 mm in diameter and 60 mm in length. The outer rubber tube was removed and the feed rods were sintered at 1200 °C for 2 h in a vertical tube furnace. After sintering, the rods were seeded in a FZ growth apparatus (FZ-T-10000-H-VI-VP) (see ESI S1) that was equipped with an infrared convergence heater using four halogen lamps and four ellipsoidal mirrors. The ZnO rod was moved upward into the furnace region at a speed of 10 mm/h while rotating at 20 rpm. The atmosphere was oxygen at 3 GPa and the total reaction time was approximately 50 minutes.

<sup>a</sup> Key Laboratory of Physics and Technology for Advanced Batteries (Ministry of Education), College of Physics, Jilin University, Changchun 130012, China.

<sup>b</sup> Laboratory for Surface Science and Technology and Department of Chemistry, University of Maine, Orono ME 04468, USA.

<sup>c</sup> College of Chemistry, Jilin University, Changchun 130012, China.

<sup>d</sup> State Key Laboratory on Integrated Optoelectronics, College of Electronic Science and Engineering, Jilin University, Changchun, 130012, China. \*Corresponding author E-mail: wpqin@jlu.edu.cn (WP. Qin) Tel: 86-431-85153853; Fax: 86-431-85168241-8325.

† Electronic Supplementary Information (ESI) available: See DOI: 10.1039/x0xx00000x

The crystal structures of the products were determined using a Rigaku D/Max-rA X-ray powder diffractometer (XRD), using a nickel-filtered Cu K $\alpha$  radiation ( $\lambda=1.5418$  Å). The size and morphology of the ZnO microrods were measured by SEM (JSM-5200 JOEL Japan). Energy dispersive X-ray (EDX) scan profiles were obtained on a JSM-5200 FESEM microscope coupled with an EDX spectrometer (Genesis Apollo XL). Raman spectra were recorded using a Horiba JY-HR-800 Raman spectrometer with an excitation wavelength of 632.8 nm. The PL spectra, at different temperatures, were recorded on a JY-U-1000 spectrometer using a LN<sub>2</sub> cooled CCD camera. The PL properties, at various excitations, were optically pumped by a Nd:YAG FHG ( $\lambda = 266$  nm, 10 Hz repetition rate, 7 ns pulse width). The pump beam was focused onto a  $\sim 20$   $\mu\text{m}$  diameter spot on the sample.

### 3. Result and discussion

#### 3.1 Structure and morphology of ZnO microrods.

Figure 1 shows the XRD spectrum of the ZnO microrods. All diffraction peaks are matched to the single crystalline wurtzite hexagonal phase of bulk ZnO (JCPDS No.79-2205). It was found that the intensity of the (100) diffraction peak at  $2\theta$  values of  $31.8^\circ$  is much stronger than other diffraction peaks, which indicates that the ZnO microrods are grown with a high orientation of their  $c$ -axis.<sup>15</sup> This is because the ZnO microrods in our work lie horizontally on the sample substrate used to record the XRD. In contrast, in the work of Park *et al.*,<sup>16</sup> the microrods were orientated perpendicular to the sample substrate and in this case, the intensity of the (002) peak was stronger than that of the other peaks. In addition, the EDX spectrum in the inset of Figure 1 shows only peaks due to zinc and oxygen.

Confirmation of the formation of ZnO is provided by Raman spectroscopy. The Raman spectrum is shown in Figure S4 of the ESI section. The Raman spectrum of the ZnO microrods is consistent with spectra reported for bulk ZnO.<sup>17, 18</sup> (See ESI S4 for details of band assignments.)

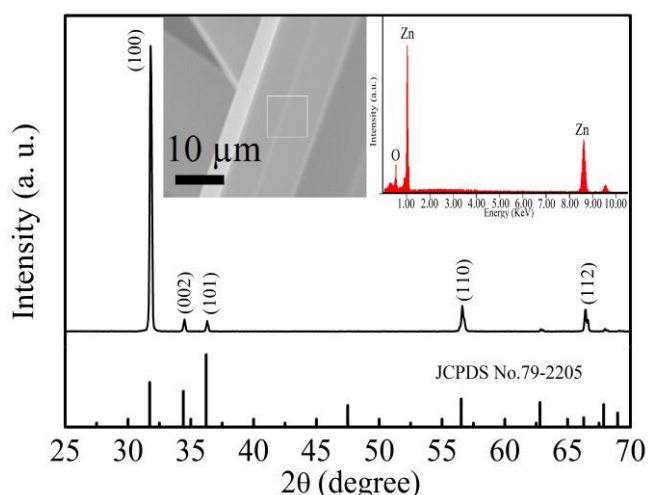


Figure 1. The XRD pattern for the ZnO microrods and the standard ZnO XRD (JCPDS No. 79-2205). The insets are the EDX spectrum of ZnO microrods and a picture that depicts the area of the sample in which the EDX was obtained.

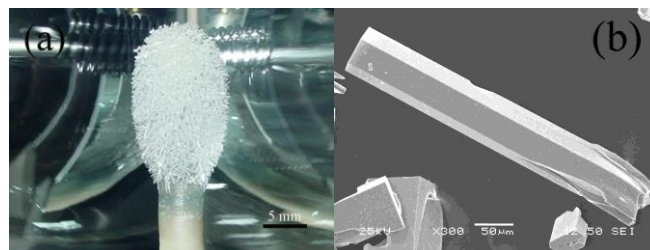


Figure 2. (a) Image of ZnO microrods (b) SEM images of one of the ZnO microrods

The size and morphology of the ZnO microrods were analyzed using digital image processing of the SEM micrograph. As shown in Figure 2(a), the ZnO microrods grown on the top of the rod have a similar appearance to the seed head of a dandelion. SEM images (see Figure 2(b)) show that one of the ZnO microrods has a hexagonal structure with a smooth surface and an aspect ratio of 9 with diameters of  $50$   $\mu\text{m}$  and lengths of about  $450$   $\mu\text{m}$ . The morphology of the ZnO microrods during their growth cycle was also monitored by observation through a window into the furnace region. (see ESI S2). It was found that the growth of the microrods was uniform and occurred by extending outward from the underlying rod in all directions, producing a final structure, as shown in Figure 2(a).

#### 3.2 Growth mechanism

Although a VLS mechanism has been widely accepted to explain ZnO growth,<sup>1, 18-20</sup> in our case, a different mechanism occurs because the temperature profile in the furnace region differs from the temperature profiles common to VLS-based methods. It is noted that despite the difference in mechanism, we obtain similar one-dimensional growth morphologies occurring in the vapor phase to that of ZnO grown using conventional VLS processes. VLS requires temperature instabilities in the furnace region in order to obtain growth of the crystals.<sup>21</sup> Typically, a solid source material is vaporized at an elevated temperature and the vapor then condenses on the top of the growing microrod that has a temperature profile extending from the surface, which leads to growth in the desired products.<sup>1</sup> In the FZ furnace used in our work, there is a temperature distribution (see ESI S3) that differs from conventional VLS furnaces in that it has a larger temperature gradient extending around the substrate. When the liquid droplets of ZnO form on the surface of the ZnO rod in the region illuminated by the 4 beams they are in equilibria with the vapor and solid phase material. The ZnO liquid droplets cool upon rotation of the rod outside of the illuminated area. At the same time, liquid droplets provide a seed for microrod growth by way of ZnO vapor deposition. The result is the growth of the ZnO microrods from the top of the liquid droplet. The light irradiation profiles from the surface of the rod to the lamp position lead to a temperature drop with distance away from the surface.<sup>22</sup> Thus, the growth of the microrod continues from the bottom of the rod, where the liquid droplet occurs. Vapor from the surrounding rod is converted to the liquid phase in the drop, providing a constant replenishment of ZnO for microrod growth to occur. Thus, this temperature profile, in combination with the rotation and movement

of the ZnO rod, results in fluctuations in temperature, which in turn, leads to the production of ZnO microrods extending outward from the surface of the underlying rod. In addition, under thermodynamic equilibrium conditions, the ZnO microrods grow preferably along the c-axis direction.<sup>23, 24</sup> This growth direction is similar for both VLS and FZ processes and hence, both lead to ZnO microrods with similar growth habit and direction.

### 3.3 Optical properties

#### 3.3.1 Excitation intensity dependent PL spectra at room temperature

The excitation intensity dependence on the PL of ZnO microrods recorded at room temperature is shown in Figure S5 of the ESI section. In general, the PL spectrum of ZnO consists of two major characteristic luminescence bands that depend on stoichiometry of the material. One is a sharp UV emission peak at  $\sim 3.145$  eV (394 nm), while the other band is relatively broader and weaker, occurring in the visible region at  $\sim 2.350$  eV (527 nm). The UV emission peak is assigned to the recombination of the free excitons of ZnO, and a peak in the visible spectral range is attributed to defect emissions.<sup>25</sup> In our case, a defect emission peak at 2.350 eV (527 nm) was observed at an excitation power density of 1-2 kW/cm<sup>2</sup>. Above the 20 kW/cm<sup>2</sup> excitation power density, a free exciton peak at 3.145 eV (394 nm) appeared, (see ESI S5(a)) and this peak dominated the PL spectrum and increased in intensity with excitation power density. (see ESI S5(b))

#### 3.3.2 PL spectra of ZnO microrods at 15 K

Figure 3 shows the PL spectrum of the ZnO microrods measured at 15 K. The most intense bands are the exciton peaks at 3.3578 eV (369.3 nm), 3.3615 eV (368.9 nm) and 3.3669 eV (368.4 nm). In a study of bulk ZnO, Reynolds *et al.*,<sup>26</sup> attributed these three emission peaks to excitons bound to neutral donors (D<sup>0</sup>X). However, the peak intensities of the particular donor-related exciton line showed differences from sample to sample.

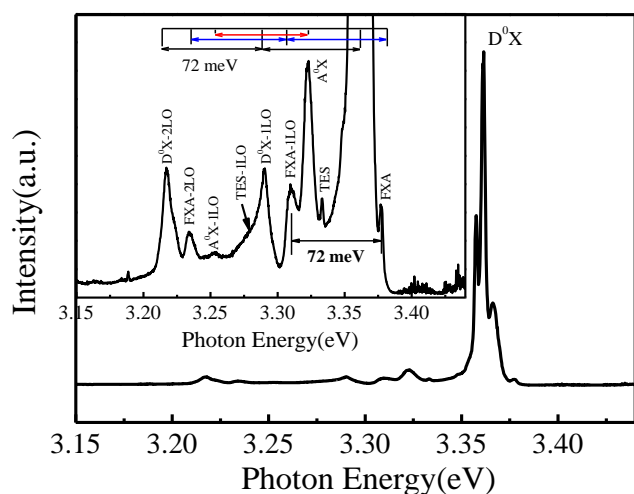


Figure 3. PL spectra of ZnO microrods at 15 K; inset shows the ordinate, amplified by a factor of 15.

For example, the most intense line was observed at 3.3628 eV by Thonke *et al.*,<sup>27, 28</sup> at 3.3624 eV by Reynolds *et al.*,<sup>26</sup> at 3.364 eV by Hamby *et al.*,<sup>9</sup> and at 3.3605 eV by Teke *et al.*,<sup>29</sup> whereas, we observed the most intense D<sup>0</sup>X at 3.3615 eV. This variation in peak position is because the concentration and capture cross section of the particular donor varies from sample to sample.<sup>29</sup> In addition, a peak of 3.3774 eV (367.2 nm) which lies on the shoulder of the D<sup>0</sup>X peak is attributed to the A-free exciton (FXA) transition.<sup>9, 30</sup> Another peak at 3.3227 eV (373 nm) is associated with acceptor-exciton (A<sup>0</sup>X) complexes and the band intensity is higher than those of excitons bound to the neutral-donor-exciton.<sup>30, 31</sup> Between the D<sup>0</sup>X and A<sup>0</sup>X peaks, lies a peak at 3.3333 eV which is lower in intensity to the main D<sup>0</sup>X peak (3.3615 eV) and lower by about 28.2 meV in energy.<sup>27</sup> This peak has been ascribed to a two-electron satellite (TES), which provides additional proof of a neutral-donor-bound exciton transition.<sup>32-34</sup>

It is noted that LO-phonon replicas occur with a separation of  $\hbar\omega_{LO} = 72$  meV, which corresponds to the LO-phonon energy in ZnO.<sup>35</sup> As a result, peaks at 3.310 eV (375 nm) and 3.235 eV (383 nm) were ascribed to a FXA-1LO and FXA-2LO transition, respectively.<sup>29</sup> The peak at 3.290 eV (377 nm), 3.217 eV (385 nm) and 3.254 eV (381 nm) are ascribed to the D<sup>0</sup>X-1LO, D<sup>0</sup>X-2LO and A<sup>0</sup>X-1LO phonon replicas, respectively.<sup>29</sup> The peak at 3.252 eV ascribed to the TES-1LO, could not be resolved due to line broadening.<sup>29</sup> The peak at 3.252 eV was ascribed to the A<sup>0</sup>X LO phonon replicas.

#### 3.3.3 Temperature-dependent PL

Since some peaks are either very weak in intensity or overlap with nearby peaks, the temperature evolution of these peaks was monitored to verify peak assignments. Figure 4 shows the near band-edge PL spectra of ZnO microrods recorded at temperatures ranging from 15 to 150 K (see ESI S6). The most intense D<sup>0</sup>X peak at 3.3615 eV (368.9 nm) quenches gradually with increasing temperature as well as the other two acceptor-related peaks at 3.3578 eV (369.3 nm) and 3.3669 eV (368.4 nm). All three peaks disappear above 120 K. The peaks, due to the D<sup>0</sup>X phonon replica at 3.2903 eV and 3.2176 eV, were present at temperatures under 60 K. When the temperature was increased above 60 K, there was a decrease in the D<sup>0</sup>X emission intensity, which was mainly due to efficient thermal quenching.<sup>9</sup> Evidence to support a quenching effect is provided by the increase in intensity of FXA and LO phonon-assisted FX peaks. The increase in intensity of the FXA and LO bands are due to an increase in the number of free excitons that are liberated by the thermal quenching of the D<sup>0</sup>X emission peak. When the temperature was raised above 30K, the TES emission peak disappeared, which was consistent with the thermal dissociation of the D<sup>0</sup>X excitons.<sup>34</sup> Another peak at 3.383 eV (366.5 nm) appears at a temperature of 60 K. Based on reported energy separation of the FXA and FXB,<sup>36, 37</sup> we assign this weak emission, that is about 9 meV higher from the FXA (for 3.374 eV (367.5 nm) at 60 K), to an FXB transition. This assignment is supported by Hamby *et al.*<sup>9</sup> which reported an energy spacing between FXA and FXB of 9 meV for bulk ZnO. The FXB

continues to increase until 120 K, above which line broadening merges the two peaks into one broad band.<sup>29</sup> Finally, above 120 K, the first, second order LO phonon replicas of the FXA line at 3.294 eV (376 nm) and 3.222 eV (385 nm) dominate the PL spectra.

A plot of the PL peak energies as a function of temperatures from 15 K to 150 K are shown in Figure 5. It is noted that the temperature variation of the FXA peak energy follows Varshni's<sup>35</sup> formula. From a fit of the curves in Figure 5 to Varshni's formula, we extrapolate the position of 3.31 eV for the FXA peak at 300 K. This is 60 meV lower than the room temperature value for the band gap of ZnO (3.37 eV), and this 60 meV is the same value reported for temperature - independent exciton binding energy.<sup>38</sup> Furthermore, the measured energy peak positions of the 1LO- 2LO phonon assisted FXA are the same values as reported in the literature for ZnO.<sup>9,29</sup>

Viswanth *et al.*<sup>39</sup> measured the intensity ratio of the FXA peak to the D<sup>0</sup>X peak, (i.e.,  $I(\text{FXA})/I(\text{D}^0\text{X})$ ) as a function of temperature) and used this to calculate the thermal activation energy in GaN. The temperature dependence of the  $I(\text{FXA})/I(\text{D}^0\text{X})$  ratio as a function of temperature is shown in Figure 6. Recall from Figure 4, that the intensity of the FXA peak increases at the expense of the D<sup>0</sup>X peak.

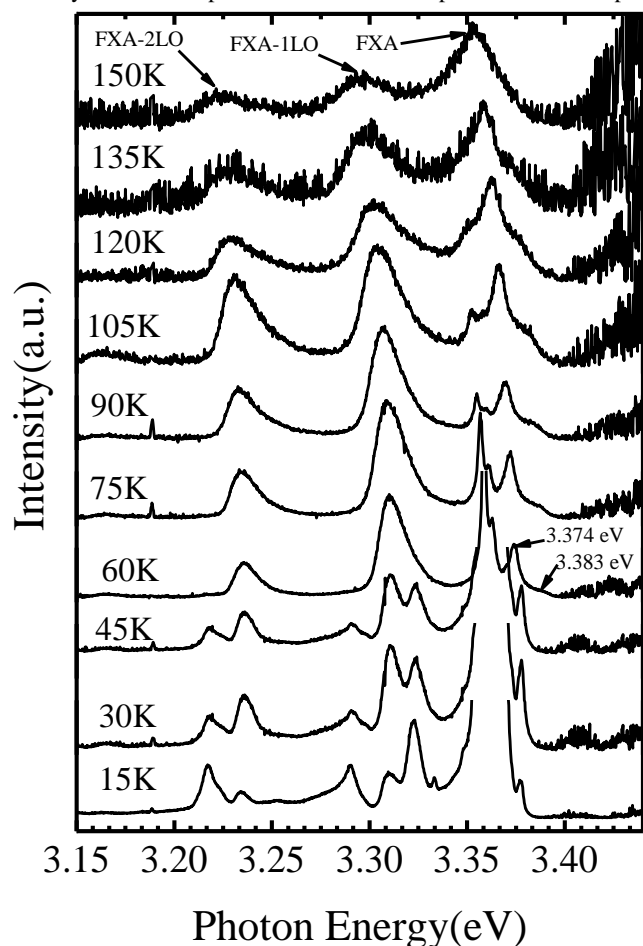


Figure 4. The PL spectra of ZnO microrods recorded at temperatures between 15 K and 150 K. Zero-, one-, and two-LO phonon-assisted FXA transitions are indicated by arrows for the 150 K spectrum and labeled as FXA, FXA-1LO, and FXA-2LO, respectively.

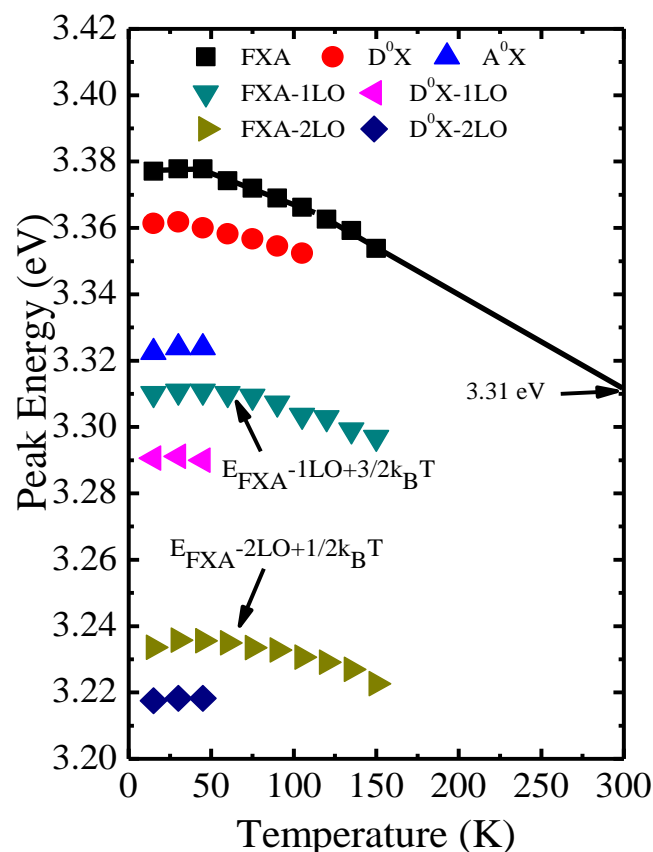


Figure 5. Peak position for PL spectra of ZnO microrods shown in Figure 4. The FXA were fit with a Varshni equation and its 1LO- and 2LO phonon replicas were fit with the equation shown in the figure. Also shown are A<sup>0</sup>X, D<sup>0</sup>X and their LO phonon replica.

Furthermore, it has been shown that the intensity of the FXA peak decreases with increasing temperature.<sup>39</sup> In Figure 6(a), the ratio increases with an increase in temperature. This behavior is similar to those reported by Hamby *et al.*<sup>9</sup> and Reynolds *et al.*<sup>26</sup> for bulk ZnO and was attributed to a dissociation of the donor bound exciton into a free exciton and a neutral donor.

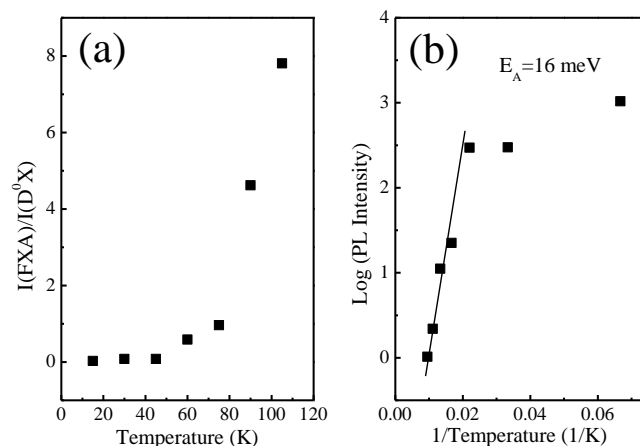


Figure 6. (a) Intensity ratio of the FXA peak to the donor bound exciton peak  $I(\text{FXA})/I(\text{D}^0\text{X})$  as a function of temperature. (b) PL intensities of the donor bound exciton as a function of  $1/T$ . The thermal activation energy of the donor bound exciton is obtained from the slope of the straight line.

Figure 6(b) is a plot of the natural logarithm of the PL intensities for the 3.3615 eV peak as a function of  $1/T$ , following the approach used by Viswanath *et al.*<sup>39</sup> for GaN and applied to bulk ZnO by Hamby *et al.*<sup>9</sup> From a fit to the linear portion of the data (first five data points), the slope gives a thermal activation energy of about 16.6 meV. This is similar to the value of 14 meV, calculated using the same procedure by Hamby *et al.* for bulk ZnO.

#### 4. Conclusions

We report the growth of ZnO microrods using a FZ method. The formation mechanism of ZnO microrods is different to the VLS mechanism because the temperature distribution is different for the two processes. The FZ method provides an approach to fabricate ZnO microrods with a diameter of micrometers and a length of the order of millimeters. At a temperature of 15 K, the PL of ZnO microrods has emission peaks assigned to the FXA, TES,  $D^0X$  transitions and its' phonon replica. The spectrum is dominated by the  $D^0X$  peak. The PL spectra for a selected temperature between 15 K and 150 K shows that the reduction in the  $D^0X$  peak intensity with increasing temperature is attributed to thermal dissociation of  $D^0X$  to FX. The PL spectrum of ZnO microrods was dominated by FX and its phonon replica with the temperature increasing above 120 K. The temperature dependent FXA energy peak was fitted to the Varshni equation and shows that the band gap of the ZnO microrods is 3.31 eV at room temperature. Following the approach of Viswanath *et al.*,<sup>39</sup> the strongest of the  $D^0X$  peaks exhibit a thermal activation energy of 16 meV, which is close to the value of 14 meV reported by Hamby *et al.*<sup>9</sup> for bulk ZnO. Such ZnO microrods can be used as test materials for studying UV lasing behavior and aid in the development of novel optical devices.

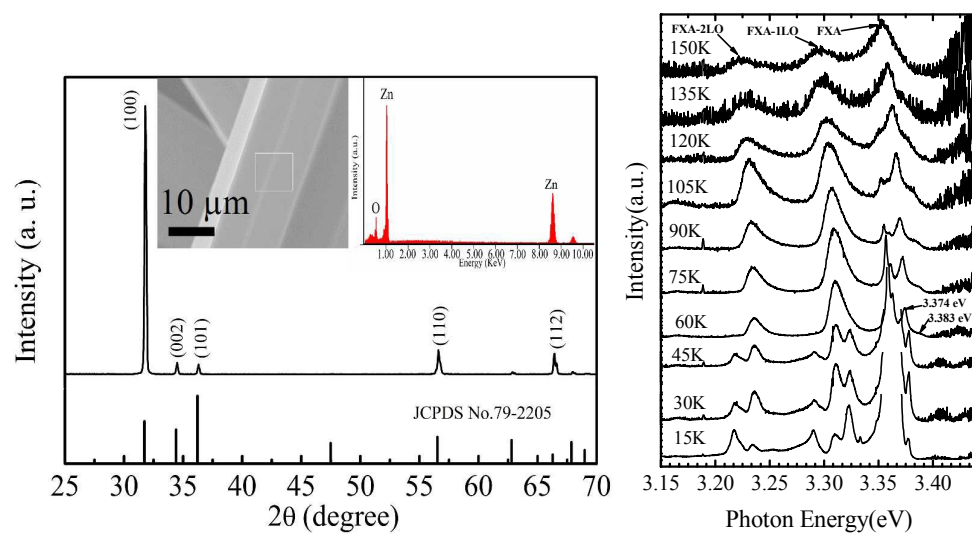
#### Acknowledgment

The authors gratefully acknowledge financial support from China Scholarship Council, This work has been financially supported by the National Natural Science Foundation of China (NSFC 11274139, 61275189, 51302103, 11474132, 11404136).

#### Notes and references

- Z. L. Wang, *J Phys-Condens Mat*, 2004, 16, R829-R858.
- H. X. Dong, Y. Liu, J. Lu, Z. H. Chen, J. Wang and L. Zhang, *J. Mater. Chem. C*, 2013, 1, 202-206.
- J. F. Lu, C. X. Xu, J. Dai, J. T. Li, Y. Y. Wang, Y. Lin and P. L. Li, *ACS Photonics*, 2015, 2, 73-77.
- C. Czekalla, T. Nobis, A. Rahm, B. Q. Cao, J. Zuniga-Perez, C. Sturm, R. Schmidt-Grund, M. Lorenz and M. Grundmann, *Phys Status Solidi B*, 2010, 247, 1282-1293.
- D. J. Gargas, M. C. Moore, A. Ni, S. W. Chang, Z. Y. Zhang, S. L. Chuang and P. D. Yang, *Acs Nano*, 2010, 4, 3270-3276.
- J. T. Li, Y. Lin, J. F. Lu, C. X. Xu, Y. Y. Wang, Z. L. Shi and J. Dai, *Acs Nano*, 2015, 9, 6794-6800.
- T. Tian, J. Xing, L. Cheng, L. Zheng, W. Ruan, X. Ruan and G. Li, *Ceram. Int.*, 2015, 41, Supplement 1, S774-S778.
- Z. Guo, H. Li, L. Zhou, D. Zhao, Y. Wu, Z. Zhang, W. Zhang, C. Li and J. Yao, *Small*, 2015, 11, 438-445.
- D. W. Hamby, D. A. Lucca, M. J. Klopstein and G. Cantwell, *J. Appl. Phys.*, 2003, 93, 3214-3217.
- Z. Y. Huang, C. F. Chai and B. Q. Cao, *Cryst. Growth Des.*, 2007, 7, 1686-1689.
- C. X. Shan, Z. Liu and S. K. Hark, *Appl. Phys. Lett.*, 2008, 92, 073103.
- R. S. Wagner and W. C. Ellis, *Appl Phys Lett*, 1964, 4, 89-90.
- J. K. Park, K. H. Kim, I. Tanaka and K. B. Shim, *J. Cryst. Growth*, 2004, 268, 103-107.
- T. Akashi, H. Iwata and T. Goto, *MATERIALS TRANSACTIONS*, 2003, 44, 802-804.
- L. Haifei, X. Xiaoliang, L. Liu, G. Maogang and L. Yansong, *J Phys-Condens Mat*, 2008, 20, 472202.
- B. J. Kwon, K. M. Lee, H. Y. Shin, J. Kim, J. Liu, S. Yoon, S. Lee, Y. H. Ahn and J. Y. Park, *Mater Sci Eng B-Adv*, 2012, 177, 132-139.
- R. Cuscó, E. Alarcón-Lladó, J. Ibáñez, L. Artús, J. Jiménez, B. Wang and M. J. Callahan, *Phys. Rev. B*, 2007, 75, 165202.
- H. J. Zhang, X. Wu, F. Y. Qu and G. G. Zhao, *Crystengcomm*, 2011, 13, 6114-6117.
- M. H. Huang, Y. Wu, H. Feick, N. Tran, E. Weber and P. Yang, *Adv. Mater.*, 2001, 13, 113-116.
- C. X. Xu, X. W. Sun, Z. L. Dong, G. P. Zhu and Y. P. Cui, *Appl. Phys. Lett.*, 2006, 88, 093101.
- T. J. Trentler, K. M. Hickman, S. C. Goel, A. M. Viano and *et al.*, *Science*, 1995, 270, 1791.
- D. Souptel, W. Löser and G. Behr, *J. Cryst. Growth*, 2007, 300, 538-550.
- W. J. Li, E. W. Shi, W. Z. Zhong and Z. W. Yin, *J. Cryst. Growth*, 1999, 203, 186-196.
- W. I. Park, D. H. Kim, S. W. Jung and G. C. Yi, *Appl. Phys. Lett.*, 2002, 80, 4232-4234.
- A. B. Djuricic, Y. H. Leung, K. H. Tam, Y. F. Hsu, L. Ding, W. K. Ge, Y. C. Zhong, K. S. Wong, W. K. Chan, H. L. Tam, K. W. Cheah, W. M. Kwok and D. L. Phillips, *Nanotechnology*, 2007, 18, 095702.
- D. C. Reynolds, D. C. Look, B. Jogai, C. W. Litton, T. C. Collins, W. Harsch and G. Cantwell, *Phys. Rev. B*, 1998, 57, 12151-12155.
- K. Thonke, T. Gruber, N. Teofilov, R. Schönfelder, A. Waag and R. Sauer, *Physica B: Condensed Matter*, 2001, 308-310, 945-948.
- B. K. Meyer, H. Alves, D. M. Hofmann, W. Kriegseis, D. Forster, F. Bertram, J. Christen, A. Hoffmann, M. Strassburg, M. Dworzak, U. Habocek and A. V. Rodina, *Phys. Status Solidi B*, 2004, 241, 231-260.
- A. Teke, Ü. Özgür, S. Doğan, X. Gu, H. Morkoç, B. Nemeth, J. Nause and H. O. Everitt, *Phys. Rev. B*, 2004, 70, 195207.
- H. C. Hsu and W. F. Hsieh, *Solid State Commun*, 2004, 131, 371-375.
- C. Klingshirn, *Phys. Status Solidi B*, 1975, 71, 547-556.
- J. S. Neal, L. A. Boatner, N. C. Giles, L. E. Halliburton, S. E. Derenzo and E. D. Bourret-Courchesne, *Nucl Instrum Meth A*, 2006, 568, 803-809.
- T. V. Butkhuizi, T. G. Chelidze, A. N. Georgobiani, D. L. Jashiashvili, T. G. Khulordava and B. E. Tsekvava, *Phys. Rev. B*, 1998, 58, 10692.
- X. H. Wang and S. J. Xu, *Appl Phys Lett*, 2013, 102, 181909.
- Y. P. Varshni, *Physica*, 1967, 34, 149-154.
- D. C. Reynolds, D. C. Look, B. Jogai, C. W. Litton, G. Cantwell and W. C. Harsch, *Phys. Rev. B*, 1999, 60, 2340-2344.
- C. Boemare, T. Monteiro, M. J. Soares, J. G. Guilherme and E. Alves, *Physica B: Condensed Matter*, 2001, 308-310, 985-988.
- Y. Chen and D. M. Bagnall, *J. Appl. Phys.*, 1998, 84, 3912.
- A. K. Viswanath, J. I. Lee, S. Yu, D. Kim, Y. Choi and C.-h. Hong, *J. Appl. Phys.*, 1998, 84, 3848-3859.

## Graphical Abstract:



The ZnO microrods are grown with a high orientation of their *c*-axis. The PL spectra of ZnO microrods at temperatures between 15 and 150 K were monitored to verify peak assignments.